

中国激光

改进的基于相位梯度最小化的相位补偿方法

董昭^{1,2,3}, 王文健¹, 王华英^{1,2,3}, 张子健¹, 王杰宇¹, 雷家良¹, 张小磊^{1*}

¹ 河北工程大学数理科学与工程学院, 河北 邯郸 056038;

² 河北省计算光学成像与光电检测技术创新中心, 河北 邯郸 056038;

³ 河北省计算光学成像与智能感测国际联合研究中心, 河北 邯郸 056038

摘要 提出了一种改进的基于相位梯度最小化的相位快速自动补偿方法。所提方法利用 Zernike 多项式拟合像差, 并将评价函数写作含多项式梯度的表达式, 采取拟牛顿法进行优化得到了对应系数, 从而实现了相位补偿。在优化过程中, 所提方法可实时给出评价函数与各多项式系数之间的导数, 有效提高了优化速度。此外, 所提方法还可利用采样技术, 进一步提高处理速度。分析和实验结果表明, 所提方法速度快、精度高, 适用于高速动态全息显微成像。

关键词 全息; 相位畸变补偿; 数字全息显微; 优化算法; Zernike 多项式

中图分类号 O436

文献标志码 A

doi: 10.3788/CJL202148.2409001

1 引言

数字全息显微术(DHM)能够实现显微物体的无标记、无损和定量相位成像, 在过去的 20 年里, 人们不断地对它进行研究^[1-5]。利用显微物镜放大衍射波时, 产生的曲率相位畸变和高阶像差会影响重建相位图像质量。Mann 等^[6-12]提出了物理或数值方法来进行相位畸变补偿。物理方法主要通过在参考光中引入相同曲率的相位畸变^[6]、远心配置^[7]和电子可调透镜^[8]等来补偿相位畸变; 或者在实验记录过程中通过调整系统的光路来消除相位像差。较为典型的物理方法是意大利 Ferraro 等^[10]提出的两步曝光法。数值方法主要在图像处理过程中进行相位补偿。Colomb 等^[11-13]提出了一种使用相位掩模的自动补偿方法, 该方法只需要一张相位图即可实现相位补偿。数值方法要求相位图存在无样品区域, 然后利用二维球面函数、多项式等对该区域进行拟合得到相位掩模, 进而实现相位补偿。深度学习的方法也被用于相位补偿, 但神经网络训练过程往往很耗时^[14]。Zuo 等^[9,15-16]提出了一种基于主成分

分析的数值补偿方法, 但该方法要求待测样品为薄样品。He 等^[17]提出了一种基于全息图自扩展的数字全息相位畸变补偿方法, 但该方法也需要无样品区域。Trujillo 等^[18-20]提出了基于定量评价指标的补偿方法, 该方法根据评价指标对参数进行调整, 从而得到补偿后的最佳相位图像。Trujillo 等^[18]引入了阈值和强度求和来表示相位畸变程度, 进而通过参数调整实现畸变补偿; Wang 等^[19]利用展开相位的极差作为补偿倾斜和曲率畸变的依据, 实现畸变补偿。这些方法都不需要相位图中存在无样品区域, 但寻找最佳参数的过程也很耗时。Liu 等^[20]提出了基于相位梯度最小化(PVM)的相位补偿方法, 该方法以包裹相位图中的梯度绝对值总变化量为判据, 利用拟牛顿法等优化算法, 在判据最小时可实现相位补偿。不过, 该方法没有在迭代中计算评价函数待优化参数的导数, 导致难以进一步提高优化速度^[21]。针对该问题, 本文改写了文献[20]中的评价函数, 在优化过程中实时计算评价函数待优化参数的导数。模拟和实验结果表明, 改进后的优化方法在保证相位补偿精度的同时, 有效提高了相位补偿效率。

收稿日期: 2021-04-23; 修回日期: 2021-05-17; 录用日期: 2021-05-24

基金项目: 河北省自然科学基金(F2018402285)、河北省高等学校科学技术研究项目(QN2020426)、邯郸市科学技术研究与发展计划(19422083008-69)

通信作者: *xiaolei6778@hebeu.edu.cn

2 分析和方法

与文献[20]类似,所提方法使用 Zernike 多项式来拟合相位畸变 φ_a 。设 P_i 为第 i 阶多项式,有

$$\varphi_a(x, y) = \sum_i a_i P_i(x, y), \quad (1)$$

式中: a_i 是第 i 阶多项式的系数。对于一组 $\{a_i\}$,如果忽略相位图中的噪声,此时样本的包裹补偿相位图可以表示为

$$\varphi_c(x, y) = [\varphi_0(x, y) - \sum_i a_i P_i(x, y)], \quad (2)$$

式中: φ_0 是实验所测原始复振幅相位; $[\cdot]$ 表示相位被包裹在 $(-\pi, \pi]$ 。一般情况下,无像差相位图相位梯度绝对值总和 $\sum_{x,y} |\nabla \varphi_c(x, y)|$ 应小于有像差情况。设由(2)式计算出的补偿后相位图为 $\varphi(x, y)$,则有

$$\sum_{x,y} |\nabla \varphi_c(x, y)| \leq \sum_{x,y} |\nabla \varphi(x, y)|. \quad (3)$$

只有当相位畸变被完全补偿时,(3)式才取等号,故可以用优化方法计算 $\sum_{x,y} |\nabla \varphi(x, y)|$ 最小时对应的 $\{a_i\}$ 值,从而实现相位补偿。 $\varphi(x, y)$ 梯度绝对值的表达式为

$$|\nabla \varphi(x, y)| = \sqrt{[\nabla_x \varphi(x, y)]^2 + [\nabla_y \varphi(x, y)]^2}, \quad (4)$$

式中: $\nabla_x \varphi(x, y)$ 为 $\varphi(x+1, y) - \varphi(x, y)$; $\nabla_y \varphi(x, y)$ 为 $\varphi(x, y+1) - \varphi(x, y)$ 。文献[20]中基于此给出的评价函数为

$$M = \sum_{x,y} \sqrt{[\nabla_x \varphi(x, y)]^2 + [\nabla_y \varphi(x, y)]^2}. \quad (5)$$

之后利用 MATLAB 等软件,基于拟牛顿法进行优化。文献[21]提供评价函数关于待优化系数的导数,即 $\frac{\partial M}{\partial a_i}$ 的值,可有效提高优化速度。然而,利用(5)式计算 $\frac{\partial M}{\partial a_i}$ 的值相当复杂,为进一步提高优化速度,所提方法对(5)式进行改写。根据文献[22],有

$$|\nabla \varphi(x, y)| = |\nabla_x \varphi(x, y)| + |\nabla_y \varphi(x, y)|. \quad (6)$$

考虑到梯度算子的线性性质,此时

$$\begin{cases} \nabla_x \varphi(x, y) = \nabla_x \varphi_0(x, y) - \sum_i a_i \nabla_x P_i(x, y) \\ \nabla_y \varphi(x, y) = \nabla_y \varphi_0(x, y) - \sum_i a_i \nabla_y P_i(x, y) \end{cases}.$$

$$(7)$$

故评价函数(5)式可以改写为

$$M = \sum_{x,y} \left| \left[\nabla_x \varphi_0(x, y) - \sum_i a_i \nabla_x P_i(x, y) \right] \right| + \sum_{x,y} \left| \left[\nabla_y \varphi_0(x, y) - \sum_i a_i \nabla_y P_i(x, y) \right] \right|. \quad (8)$$

在优化过程中, $\nabla \varphi_0$ 和 ∇P_i 保持不变,可有效降低计算量,甚至可以进行抽样计算。此时 M 关于 $\{a_i\}$ 的导数为

$$\begin{aligned} \frac{\partial M}{\partial a_i} = & \sum \left(\frac{\partial |\nabla_x \varphi_0|}{\partial [\nabla_x \varphi_0]} \cdot \frac{\partial [\nabla_x \varphi_0]}{\partial (\nabla_x \varphi_0)} \cdot \frac{\partial (\nabla_x \varphi_0)}{\partial a_i} \right) + \\ & \sum \left(\frac{\partial |\nabla_y \varphi_0|}{\partial [\nabla_y \varphi_0]} \cdot \frac{\partial [\nabla_y \varphi_0]}{\partial (\nabla_y \varphi_0)} \cdot \frac{\partial (\nabla_y \varphi_0)}{\partial a_i} \right). \end{aligned} \quad (9)$$

对于一个角 φ , $[\varphi] = \varphi - n \cdot 2\pi$, 因此 $\partial [\varphi]/\partial \varphi = 1$, 故

$$\frac{\partial M}{\partial a_i} = \sum \{ \text{sgn}([\nabla_x \varphi_0]) \cdot \nabla_x P_i + \text{sgn}([\nabla_y \varphi_0]) \cdot \nabla_y P_i \}, \quad (10)$$

式中: $\text{sgn}(\cdot)$ 是符号函数。这里的非线性优化问题可以表示为

$$(\hat{a}_1, \hat{a}_2, \dots) = \arg \min M(a_1, a_2, \dots). \quad (11)$$

式中: \hat{a}_i 表示优化后的参数值。之后利用 MATLAB 中的 fminunc 函数,用拟牛顿法和(8)式以及(10)式来实现优化过程,得到的系数可用于展开(2)式,得到补偿相位。本项工作使用软件 MATLAB 2018a,在 2.50 GHz 的 Intel Core i7-6500U CPU 和 8G RAM 的笔记本计算机上完成。

3 结果与讨论

首先,利用仿真模拟手段检验所提改进的 PVM 相位补偿方法。样品的相位值固定为 0,大小为 512 pixel \times 512 pixel。相位畸变采用 1~9 阶 Zernike 多项式模拟,这些多项式的表达式可参考文献[20],对应的设定系数如表 1 所示。图 1(a)为包裹后的畸变相位图,图 1(b)为文献[20]所列原始方法补偿的相位图。两种方法参数中 $\{a_i\}$ 的初始值相同,均设为 0,所提方法补偿后的相位图如图 1(c)所示。从表 1 中可以看出,所提方法得到的系数在保留 4 位小数的情况下与设定值相同,而原始 PVM 方法得到的系数则在万分位与设定值有所差异。图 1 也表明在精度为 10^{-3} rad 时,原始方法保留的相位畸变更大。上述结果表明,所提方法比原始方法精度更高,主要原因在于 MATLAB 设置的最大迭代次数为 900 次,在没有提供评价函数关于待优化参数导数时,原始方法难以收敛。所提改进后的

表1 模拟中 Zernike 多项式系数

Table 1 Coefficients of Zernike polynomial in simulations

P_i	Set value	a_i		
		Original PVM	Improved PVM	Sampling PVM
Z_1	15.0000	14.9996	15.0000	15.0000
Z_2	-10.0000	-10.0008	-10.0000	-10.0000
Z_3	20.0000	19.9997	20.0000	20.0000
Z_4	0.5000	0.5002	0.5000	0.5000
Z_5	-0.3000	-0.3000	-0.3000	-0.3000
Z_6	0.5000	0.5001	0.5000	0.5000
Z_7	0.0000	0.0001	-0.0000	-0.0000
Z_8	-0.5000	-0.4999	-0.5000	-0.5000
Z_9	0.5000	0.5001	0.5000	0.5000

^a1% of the pixels are selected by uniform sampling

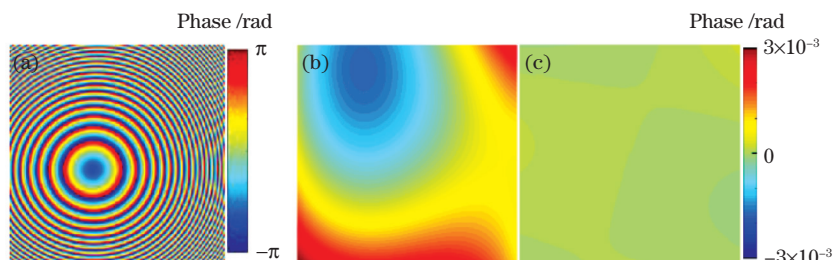


图1 模拟结果。(a)仿真的畸变相位图;(b)原始PVM方法补偿的相位图;(c)改进后PVM方法补偿的相位图

Fig. 1 Simulation results. (a) Distorted phase map in simulation; (b) phase diagram compensated by original PVM method; (c) phase diagram compensated by improved PVM method

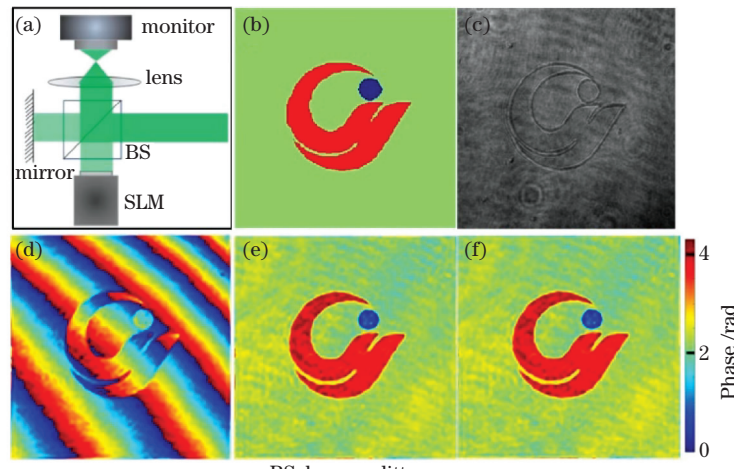


图2 空间光调制器加载相位图的实验结果。(a)Michelson 干涉成像平面示意图;(b)空间光调制器生成的相位图;(c)接收的全息图;(d)重构的未补偿包裹相位图,色标与图1(a)相同;(e)改进后 PVM 方法补偿的相位图;(f) 原始 PVM 方法补偿的相位图,图2(b)、(e)、(f)有相同的色标

Fig. 2 Experimental results of loading phase diagram of spatial light modulator. (a) Schematic diagram of Michelson interferometry image plane; (b) phase map produced by SLM; (c) received hologram; (d) reconstructed uncompensated wrapped phase map, its color bar is the same as Fig. 1(a); (e) phase diagram compensated by improved PVM method; (f) phase diagram compensated by original PVM method, Figs. 2(b), (e), (f) have the same color bar

方法完成优化过程大约需要 2.00 s(约需 100 次迭代),原始方法大约需要 10.60 s 才能完成 900 次迭代,说明所提方法可有效提高运算速度。

同时也对所提改进的 PVM 方法进行了测试。实验使用的仪器为反射式空间光调制器(SLM, 型号 HRSLSM84R, 上海瑞立柯公司)。图 2(a)为 Michelson 干涉光路图;图 2(b)为 SLM 生成的相位图;图 2(c)和图 2(d)为接收到的全息图和大小为 512 pixel×512 pixel 的未补偿重构相位图;图 2(e)和图 2(f)分别是改进后 PVM 方法和原始 PVM 方法补偿的相位图。图 2(e)和图 2(f)均与图 2(b)匹配得非常好,这意味着基于相位梯度最小化的两种方法在实际应用中都是准确的。但原始方法完成优化大约需要 2.544 s,而改进后的方法完成优化大约需要 0.536 s,后一种方法效率更高。

使用数字全息显微实验得到的含曲率相位畸变的相位图来检验所提方法。实验装置参考文献[19]。图3(a)是所得血细胞全息图,图3(b)是所得待补偿包裹相位图;图3(c)和图3(d)分别是改进后PVM方法和原始PVM方法补偿后的包裹相位图;图3(e)和图3(f)分别为对应的解包裹相位图。这两种方法对倾斜畸变和曲率畸变均进行了补偿。采用结构相似度指数(SSIM)^[23]定量表示它们的相似度,图3(e)和图3(f)之间的值为0.9999,说明两种方法解包裹

效果是一致的,但是原始方法和所提改进方法的处理时间分别为2.049 s和0.398 s,后者比前者快了5倍。拟牛顿法在优化过程中需要不断计算 $\partial M / \partial a_i$ 的值,以调整参数 a_i 的优化方向。如未能提供它,程序将通过微分数值计算方法,即通过参数 a_i 变化一个小量 δ_i 来观察相应M值的变化^[21]。这不仅增加了运算量,计算精度也受 δ_i 值的影响,最终增加了运算时间。由于所提改进后的PVM方法能精确提供 $\partial M / \partial a_i$ 的值,运算效率得以明显提高。

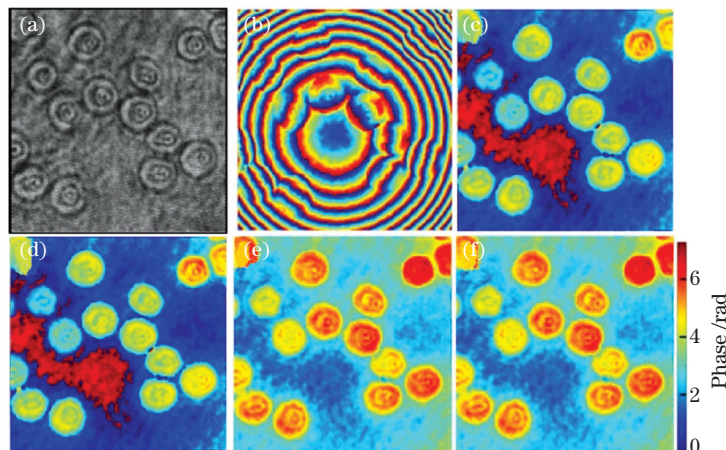


图3 血红细胞的实验结果。(a)血细胞全息图;(b)重构的未补偿包裹相位图;(c)改进PVM方法补偿的包裹相位图;(d)原始PVM方法补偿的包裹相位图;(e)图3(c)对应的解包裹相位图;(f)图3(d)对应的解包裹相位图,图3(c)和图3(d)的色标与图1(a)相同,图3(e)和图3(f)有相同的色标

Fig. 3 Experimental results of red blood cells. (a) Hologram of blood cells; (b) reconstructed uncompensated wrapped phase map; (c) wrapped phase diagram compensated by improved PVM method; (d) wrapped phase diagram compensated by original PVM method; (e) corresponding unwrapped phase map of Fig. 3(c); (f) corresponding unwrapped phase map of Fig. 3(d), color bar of Fig. 3(c) and Fig. 3(d) is the same as Fig. 1(a), Figs. 3(e) and Fig. 3(f) have the same color bar

采用(7)式作为评价函数后,优化速度较文献[20]的原始方法还可进一步提高。由于相位梯度是一个低频线性信号,相关的多项式也是低频的,根据Shannon采样定理^[24],通过抽样方法仅需少许数据点便可拟合相位畸变。采用均匀采样的方法从图像中选取1%的点,然后利用改进后的PVM方法进行

相位补偿。此抽样PVM方法所得结果如图4所示,图4(a)为对应图1(a)的补偿解包裹相位图。仿真结果表明,抽样PVM方法也具有较高的精度,补偿时间为0.079 s;抽样与PVM方法相比大约节省了96%的处理时间。

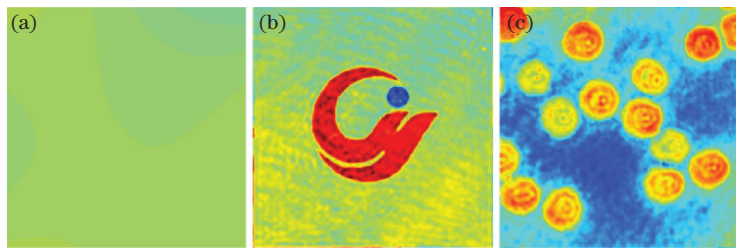


图4 抽样PVM方法得到的补偿解包裹相位图。(a)对应图1(a)的补偿解包裹相位图;(b)对应图2(d)的补偿解包裹相位图;(c)对应图3(b)的补偿解包裹相位图,色标分别与图1(b)、图2(e)和图3(e)相同

Fig. 4 Compensated unwrapped phase map obtained by sampling PVM method. (a) Compensated unwrapped phase diagram corresponding to Fig. 1 (a); (b) that of Fig. 2 (d); (c) that of Fig. 3 (b), their color bars are the same as Fig. 1(b), Fig. 2(e), and Fig. 3(e), respectively

为了检验抽样 PVM 方法在实际应用中的鲁棒性, 使用了该方法对图 2(d) 和图 3(b) 进行补偿, 图 4(b) 和图 4(c) 分别为对应的未包裹补偿相位图。图 4(b) 与图 2(e) 之间的 SSIM 为 0.9981, 图 4(c) 与图 3(e) 之间的 SSIM 为 0.9870, 表明在相同条件下抽样 PVM 方法可以和未抽样 PVM 方法一样精确。图 2(b) 和图 3(b) 补偿的处理时间分别为 0.085 s 和 0.074 s, 与不经采样的改进 PVM 方法相比, 采样后进一步节省了 84% 和 81% 的处理时间。

Liu 等^[25] 指出 PVM 方法对噪声敏感。PVM 方法无法完全将由散斑等噪声引起的局部相位畸变去除, 如图 2(e)、(f) 所示。更精确的结果往往需要在已有初步结果的基础上, 再采用其他方法来做进一步相位补偿。如文献[25]就采用两步拟合的方法得到细胞的补偿相位图, 但该方法又需要无样品区域; 文献[26]利用正交多项式构造的数字相位掩模分区域对相位像差进行了建模, 虽然提高了抗噪性能, 但大大增加了运算时间。在实际工作中, 为了保证成像质量, 在图像采集和提取相位过程中往往需要去噪措施, 如所提 PVM 方法在测量中使用隔振台隔振等常规去噪手段。测试结果表明, 所提 PVM 方法此时就能得到较为准确的补偿结果, 但如何进一步去除散斑等噪声等造成的局部相位畸变仍是一个值得研究的课题。

4 结 论

提出了一种改进后的基于梯度最小化的相位补偿方法, 该方法可实现自动快速相位补偿。通过对文献[20]中的评价函数进行适当处理, 在优化过程中实时给出了该函数与待优化系数的导数, 有效提高了拟牛顿法优化速度。仿真和实验结果表明, 所提方法可以在保证精度的前提下, 明显提高运算效率。基于改进后的评价函数, 通过采样的方法进一步缩短了处理时间。分析和实验结果也表明, 采样方法也能在一般测量中保证处理精确度。所提相位补偿方法可用于动态全息显微成像等快速成像场合。

参 考 文 献

- [1] Cuche E, Bevilacqua F, Depeursinge C. Digital holography for quantitative phase-contrast imaging [J]. Optics Letters, 1999, 24(5): 291-293.
- [2] Dai S Q, Dou J Z, Zhang J W, et al. Digital holography based near-field imaging and its application[J]. Acta Optica Sinica, 2020, 40(1): 0111008.
- [3] Wen K, Ma Y, Zhang M L, et al. Quantitative phase microscopy with high stability [J]. Laser & Optoelectronics Progress, 2020, 57(20): 200001.
- [4] Psota P, Mokrý P, Lédl V, et al. Image plane digital holographic microscope for the inspection of ferroelectric single crystals[J]. Optical Engineering, 2016, 55(12): 121731.
- [5] Feng F, Tian A L, Liu B C, et al. Full-field three-dimensional test for scratch defects using digital holographic scanning imaging system [J]. Chinese Journal of Lasers, 2020, 47(4): 0409003.
- [6] Mann C, Yu L, Lo C M, et al. High-resolution quantitative phase-contrast microscopy by digital holography [J]. Optics Express, 2005, 13(22): 8693-8698.
- [7] Deng D, Peng J, Qu W, et al. Simple and flexible phase compensation for digital holographic microscopy with electrically tunable lens[J]. Applied Optics, 2017, 56(21): 6007-6014.
- [8] Ebrahimi S, Dashtdar M, Sánchez-Ortiga E, et al. Stable and simple quantitative phase-contrast imaging by Fresnel biprism [J]. Applied Physics Letters, 2018, 112(11): 113701.
- [9] Zuo C, Chen Q, Qu W J, et al. Phase aberration compensation in digital holographic microscopy based on principal component analysis[J]. Optics Letters, 2013, 38(10): 1724-1726.
- [10] Ferraro P, de Nicola S, Finizio A, et al. Compensation of the inherent wave front curvature in digital holographic coherent microscopy for quantitative phase-contrast imaging [J]. Applied Optics, 2003, 42(11): 1938-1946.
- [11] Colomb T, Cuche E, Charrière F, et al. Automatic procedure for aberration compensation in digital holographic microscopy and applications to specimen shape compensation [J]. Applied Optics, 2006, 45(5): 851-863.
- [12] Di J L, Zhao J L, Sun W W, et al. Phase aberration compensation of digital holographic microscopy based

- on least squares surface fitting[J]. Optics Communications, 2009, 282(19): 3873-3877.
- [13] Gao C, Wen Y F, Cheng H B, et al. Automatic phase-distortion compensation algorithm in digital holography[J]. Acta Optica Sinica, 2018, 38(12): 1209001.
高超, 文永富, 程灏波, 等. 数字全息中的自动相位畸变补偿算法 [J]. 光学学报, 2018, 38 (12): 1209001.
- [14] Nguyen T, Bui V, Lam V, et al. Automatic phase aberration compensation for digital holographic microscopy based on deep learning background detection[J]. Optics Express, 2017, 25(13): 15043-15057.
- [15] Sun J, Chen Q, Zhang Y, et al. Optimal principal component analysis-based numerical phase aberration compensation method for digital holography [J]. Optics Letters, 2016, 41(6): 1293-1296.
- [16] Zhang X Y, Sun J S, Zhang Z X, et al. Multi-step phase aberration compensation method based on optimal principal component analysis and subsampling for digital holographic microscopy [J]. Applied Optics, 2019, 58(2): 389-397.
- [17] He W L, Liu Z J, Yang Z M, et al. Robust phase aberration compensation in digital holographic microscopy by self-extension of holograms [J]. Optics Communications, 2019, 445: 69-75.
- [18] Trujillo C, Castañeda R, Piedrahita-Quintero P, et al. Automatic full compensation of quantitative phase imaging in off-axis digital holographic microscopy [J]. Applied Optics, 2016, 55(36): 10299-10306.
- [19] Wang H Y, Dong Z, Wang X, et al. Phase compensation in digital holographic microscopy using a quantitative evaluation metric[J]. Optics Communications, 2019, 430: 262-267.
- [20] Liu S, Lian Q, Qing Y, et al. Automatic phase aberration compensation for digital holographic microscopy based on phase variation minimization [J]. Optics Letters, 2018, 43(8): 1870-1873.
- [21] Optimization toolbox user's guide MATLAB R2018a [M]//Coleman T F, Zhang Y. Natick: The Mathworks Inc, 2018: 6-7.
- [22] Gonzalez R C, Woods R E. Digital imaging processing [M]. 3rd ed. Beijing: Publishing House of Electronics Industry, 2017.
- [23] Wang Z, Bovik A C, Sheikh H R, et al. Image quality assessment: from error visibility to structural similarity [J]. IEEE Transactions on Image Processing, 2004, 13(4): 600-612.
- [24] Lü N G. Fourier optics [M]. 2nd ed. Beijing: China Machine Press, 2006: 57-62.
吕乃光. 傅里叶光学 [M]. 2 版. 北京: 机械工业出版社, 2006: 57-62.
- [25] Liu S, Lian Q S, Xu Z P. Phase aberration compensation for digital holographic microscopy based on double fitting and background segmentation [J]. Optics and Lasers in Engineering, 2019, 115: 238-242.
- [26] Liu S, Zhu W Z, Xu Z P, et al. Automatic and robust phase aberration compensation for digital holographic microscopy based on minimizing total standard deviation [J]. Optics and Lasers in Engineering, 2020, 134: 106276.

Improved Phase Compensation Method Based on Phase Vibration Minimization

Dong Zhao^{1,2,3}, Wang Wenjian¹, Wang Huaying^{1,2,3}, Zhang Zijian¹,
Wang Jieyu¹, Lei Jiali, Zhang Xiaolei^{1*}

¹ School of Mathematics and Physics Science and Engineering, Hebei University of Engineering, Handan, Hebei 056038, China;

² Hebei Computational Optical Imaging and Photoelectric Detection Technology Innovation Center,
Handan, Hebei 056038, China;

³ Hebei International Joint Research Center for Computational Optical Imaging and Intelligent Sensing,
Handan, Hebei 056038, China

Abstract

Objective This work presents an improved phase vibration minimization (PVM)-based method for fast compensating phase aberrations in digital holographic microscopy. Polynomials are used to fit the aberrations, and the quasi-Newton optimization procedure is applied to find their coefficients. During the optimization procedure, gradients of the merit function value related to the coefficients are offered. The results of simulations and

experiments show that this treatment makes the procedure fast and more reliable. Furthermore, the sampling technique is used to improve the processing speed even further. The analysis and experimental results reveal the improved method that can meet the demand for robustness to noise in everyday use. With high speed and accuracy, this method is suitable for dynamic holographic microscopic imaging.

Methods This work presents an improved PVM-based method for fast compensating phase aberrations in digital holographic microscopy. We use polynomials, such as standard and Zernike polynomials, to fit the phase aberration φ_a . To further improve the optimization speed, formula (4) is rewritten. The rewritten formula is shown in formula (7). It is more convenient to use software such as MATLAB to compute the derivative of the optimization coefficient and then use the fminunc function in MATLAB to carry out the optimization process using the quasi-Newton method and evaluation function (7). The obtained aberration coefficient $\{a_i\}$ can expand the formula (2) to obtain the compensated phase. In addition, this method can conveniently use sampling technology to increase the processing speed further.

Results and Discussions Simulative methods are used to verify the gradient-offered PVM-based method. This method is more accurate than the original method (Table 1). The main reason is that the maximum number of iterations set by MATLAB is 900. When the derivative of the optimized function with respect to the parameter to be optimized is not provided, the original method's calculation process fails to converge. The improved method in this paper completes the optimization process in about 2.00 s (approximately 100 iterations), whereas the original method takes about 10.60 s to complete 900 iterations (Figs. 1 and 2). This demonstrates that the improved PVM method can significantly speed up the calculation. Moreover, we used experimental methods to test the improved PVM method (Fig. 3). However, the original method takes about 2.544 s to complete the optimization, whereas the improved method takes about 0.536 s. The latter method is more efficient. The improved PVM method with sampling processing can save the processing time (Fig. 4). Compared to the improved PVM method without sampling, sampling saves 84% and 81% of the processing time.

Conclusions The PVM-based method can accomplish phase compensation without the need for specimen-free areas. In this paper, we introduce the gradients of the merit function value M related to $\{a_i\}$ in the method's nonlinear optimization process by properly processing the merit function. It becomes faster and more reliable with this treatment, according to simulation and experimental results. Furthermore, sampling can be used to reduce processing time even further. Analysis and experimental results show that the improved PVM method and that with the sampling can meet the demand for noise robustness in common use. With high speed and accuracy, the improved PVM-based methods can be used in dynamic holographic microscopic imaging.

Key words holography; phase distortion compensation; digital holographic microscopy; optimization algorithm; Zernike polynomial

OCIS codes 090.1000; 090.1995